Bedload monitoring under conditions of ultra-high suspended sediment concentrations

Frédéric Liébault, Hugo Jantzi, S Klotz, J B Laronne, Alain Recking

Journal of Hydrology xxx (2016) xxx–xxx

Contents lists available at ScienceDirect

Journal of Hydrology

journal homepage: www.elsevier.com/locate/jhydrol

Research papers

Bedload monitoring under conditions of ultra-high suspended sediment concentrations

F. Liébault [a,*], H. Jantzi [a], S. Klotz [a], J.B. Laronne [b], A. Recking [a]

[a] Université Grenoble Alpes, Irstea, UR ETNA, 2 rue de la Papeterie, BP76, F-38402 Saint-Martin-d'Hères, France
[b] Department of Geography & Environmental Development, Ben Gurion University of the Negev, Beer Sheva, Israel

ARTICLE INFO

Article history:
Received 5 February 2016
Received in revised form 23 May 2016
Accepted 8 July 2016
Available online xxxx
This manuscript was handled by Tim McVicar, with the assistance of Nikolaus Callow, Associate Editor

Keywords:
Bedload monitoring
Reid bedload slot sampler
Mediterranean badlands
Gully
Ultra-high suspended sediment concentration
Draix observatory

ABSTRACT

The bedload response of the Moulin Ravine, a small alluvial system draining a very active Mediterranean badlands landscape entrenched into Jurassic black marls of the Southern French Prealps, has been investigated using an automatic Reid bedload slot sampler. This site is known for its exceptional sediment transport conditions thanks to a long-term monitoring program that started in the late 1980s, revealing a mean annual bedload yield of 2810 t km^{-2} yr^{-1}, and suspended sediment concentrations (SSCs) during flow events commonly reaching 100 g L^{-1}. With the deployment of the slot sampler, it has been possible to record instantaneous bedload fluxes during 10 s time increments and to investigate bedload response under flow conditions with ultra-high SSCs. Bedload records cover 4 flashy summer flow events induced by heavy convective storms including a 20-yr return period event. Due to the very high SSC conditions these events challenge bedload monitoring. Even if slot sampling has been recognized as insensitive to fine sediments (silts and clays), it has never been tested in such exceptional muddy flow conditions. The bedload slot sampler performed well in such conditions. A flow-invariant proportion of fines (~15–20%) was captured in the slot sampler during flows. This proportion is equivalent to its content in the active bedload layer during summer flows, suggesting that fines enter the slot embedded with coarse particles. Instantaneous bedload fluxes recorded in the Moulin are amongst the highest hitherto reported values worldwide, providing evidence of the exceptional sediment transport conditions of marly alpine badlands. The dimensionless entrainment threshold is one order of magnitude higher than commonly reported for gravel-bed rivers, likely reflecting the cohesion effect of fines intruded in the channel surface and subsurface.

1. Introduction

Mediterranean marly badlands (e.g., badlands developed in marls, a consolidated mudstone) are recognized as one of the most erosive landscapes on earth, due to the combination of steep slopes, soft rocks, low vegetation cover and high frequency of heavy storms (Descroix and Mathys, 2003; Nadal-Romero et al., 2011). Although they are often mentioned as major sources of fine-grained suspended sediments with associated problems of reservoir sedimentation or river channels clogging by silts and clays (e.g., Owens et al., 2005; Verstraeten et al., 2006; Navratil et al., 2012), they have not been investigated as very efficient bedload conveyors. Although the contribution of bedload to the total sediment yield of marly badlands has been mentioned (e.g., Mathys et al., 2003; Garcia-Ruiz et al., 2008), our knowledge about the bedload response of such landscapes with respect to flow conditions is still very limited. It has been hitherto based on time-integrated bedload yields at the scale of single or multiple flow events, obtained from topographic resurveys of sediment retention basins. Such data are useful for a first-order assessment of the bedload contribution to sediment yield, but the resolution is too low to investigate properties of the bedload response, such as entrainment thresholds or the dependence of unit bedload flux on the average shear stress acting upon the bed.

At the erosion observatory of Draix, a long-term field observatory of erosion and hydrological processes in the Southern French Prealps, a high-frequency bedload monitoring program was initiated in late 2011 to investigate the bedload response to flow conditions in highly erosive marly badlands. This monitoring program is intended to provide the first high-resolution dataset on bedload fluxes for this kind of harsh environment, characterized by ultra-high suspended sediment concentrations (SSC) during regular flow events, often about 100 g L^{-1} and reaching maximum values about

* Corresponding author.
E-mail address: frederic.liebault@irstea.fr (F. Liébault).

http://dx.doi.org/10.1016/j.jhydrol.2016.07.014
0022-1694/

400 g L^{-1} (Mathys et al., 2003). Previous attempts to sample bedload transport in such muddy flows are very rare; the only reported case is the sediment transport study of a river draining Mount Pinatubo after the 1991 eruption, including direct bedload measurements with a Helley-Smith sampler (Hayes et al., 2002). However, this dataset is restricted to wadable flow conditions with high (ca. 40–80 g L^{-1}) but not ultra-high SSCs. Bedload responses during muddy flows are also regularly monitored in ephemeral desert channels of Israel since the early 1990s using automatic slot samplers (Laronne and Reid, 1993; Cohen et al., 2010), where average and maximum SSCs are about 40 and 200 g L^{-1}, respectively. Although it is recognized that slot samplers are insensitive to entry of fine particles (Poreh et al., 1970), exceptional suspended sediment transport conditions at Draix challenges bedload monitoring with slot samplers. It is notably uncertain that the separation between fine and coarse-grained sediments during transport will be as efficient as previously demonstrated by various slot samplers testing in different environmental settings (e.g., Laronne et al., 2003 for a review).

The three main objectives of this study are:

(i) to document instantaneous bedload transport rates in conditions of ultra-high SSC and a shallow flow regime using an automatic Reid (previously termed Birkbeck) bedload slot sampler;
(ii) to evaluate if the sampler is sensitive to fine-grained sediments under conditions of ultra-high SSC by inspection of the grain-size composition of the mass deposited in the sampler;
(iii) to characterize the bedload response to hydraulic forcing dependent on SSC, as well as incipient motion conditions for bedload in such rapidly eroding landscapes. Which specific bedload response of gully ravines can we expect under the effect of very high SSC, and do they behave similarly to previously documented very high bedload fluxes?

2. The Moulin Ravine at Draix

The Moulin Ravine drains a 8.9 ha upland Mediterranean catchment entrenched in Jurassic black marls of the Southern Prealps, in SE France near Digne-les-Bains (midpoint at 44°08′32″N, 6°21′42″E; Fig. 1). The catchment, with elevations between 850 and 925 m a.s.l., is part of the long-term erosion observatory of Draix in Haute-Provence, which has been operating since the early 1980s in a set of experimental catchments with contrasted size and forest cover (Mathys et al., 2003). Alpine black marls, a consolidated mudstone, are known to be prone to active gullying erosion (Antoine et al., 1995), resulting in a typical V-shaped badlands relief (Fig. 2A) eroding at a rate of ~1 cm yr^{-1} at Draix (Mathys, 2006). This rapidly eroding landscape is subject to a mountainous Mediterranean climate, with a mean annual rainfall of ~900 mm, and 10.9 °C mean annual temperature (since the early 1980s). The largest flow events in the ravines generally occur during late spring and summer under the effect of convective storms (Fig. 2B), and occasionally during autumn. The seasonal distribution of rainfall is typical of a Mediterranean climate, with one major peak in autumn and a secondary peak during spring.

Sediment transport monitoring in the Moulin Ravine started in 1988, with the construction of a 215 m^3 sediment retention basin and the deployment of a gauging station equipped with a turbidimeter and an automatic 24-bottle ISCO water sampler for monitoring suspended sediment (Fig. 1). Before the deployment of the automatic bedload sampler in late 2011, bedload transport was evaluated by event-based topographic resurveys of the sediment retention basin. Based on the 26 yr record of sediment transport in this catchment, the mean annual bedload yield is 2810 t km^{-2} yr^{-1}, which represents about half of the total sediment yield inclusive of suspended load, monitored at one gauging station of the Moulin (Mathys, 2006). Solutes are not monitored and therefore, are not included in the total yield. SSC during floods can reach several hundreds of grams per liter (Mathys et al., 2003), a rarely reported value in the literature with exceptions such as for the Loess Plateau of China (Gao et al., 2015), loess in Indian arid zone (Sharma, 1996), the semi-arid to arid areas in Israel (Gerson, 1977; Schick and Lekach, 1993; Alexandrov et al., 2007, 2009), and marly badlands of the Spanish Pyrenees (Garcia-Ruiz et al., 2008). These peak concentrations are generally observed during spring and summer convective storms, especially during the first flush (Mathys, 2006).

The bedload sampler was deployed about 10 m upstream from the sediment retention basin, at the head of a straight embanked trapezoidal channel. The approach reach of the sampler is a hillslope-confined alluvial channel with a riffle-pool-bar morphology (Fig. 3A), characterized by a mean channel slope of 0.045, a mean bankfull width and depth of 2.7 and 0.5 m, respectively, and a mean surface D_{50} of 2 mm. A concrete weir was constructed across the entire channel reach from the sampler downstream to ensure that the slot is always flush with the bed. This modification of the natural channel is required for bedload monitoring with a permanent slot sampler.

3. Material and methods

3.1. Bedload monitoring

Reid-type automatic bedload samplers have been recognized as the most reliable apparatus for the direct unmanned and continuous sampling of bedload during floods (Laronne et al., 2003). Since the pioneering field experiment of Turkey Brook in the UK (Reid et al., 1980), this technique has been successfully used in a variety of fluvial environments, including humid (Garcia et al., 2000), hyper-arid (Cohen and Laronne, 2005), and semi-arid (Laronne and Reid, 1993) gravel-bed streams, as well as a 40-m wide alpine river (Habersack et al., 2001) and a 1.2-m wide sandy braided channel (Lucia et al., 2013). Bedload samplers have also been recently used to calibrate leading-edge acoustic bedload monitoring systems (Mizuyama et al., 2010; Rickenmann et al., 2014). A comprehensive description of the measuring principle can be found in several reference papers (Reid et al., 1980; Laronne et al., 2003), and therefore only a brief overview is presented here. The sampler operates as a device which continuously weighs the mass of bedload accumulating in a bed excavation after having fallen into a slot flush with the bed. Sediment is deposited in a box positioned over a load cell or a water-filled pressure pillow connected to a vented pressure transducer. A second independent vented pressure transducer records the hydrostatic pressure and thus allows isolating the pressure response associated with bedload deposition in the box from the hydrostatic pressure.

The bedload sampler deployed in the Moulin Ravine has a 0.34 m^3 capacity (corresponding to ~440 kg, given a measured bulk sediment density of 1.3). The actual value of the full capacity is slightly smaller than the total volume of the inner box, because the slot opening prevents complete filling of sediment to the brim of the box. The sampler is equipped with a rubber pressure pillow and two vented Druck transducers having a precision of 1.2 mm (0.04% of the 300 mbar full scale). The vendor-specified sensor precision gives a mass resolution of 1.33 kg (95% confidence interval). This value was used as the critical level of detecting cumulative sediment deposition in the inner box. A chain-and-pulley system is used to lift the inner box for sampling and cleaning operations. The stainless steel inner box was designed with a side-wall door

Please cite this article in press as: Liébault, F., et al. Bedload monitoring under conditions of ultra-high suspended sediment concentrations. J. Hydrol. (2016), http://dx.doi.org/10.1016/j.jhydrol.2016.07.014

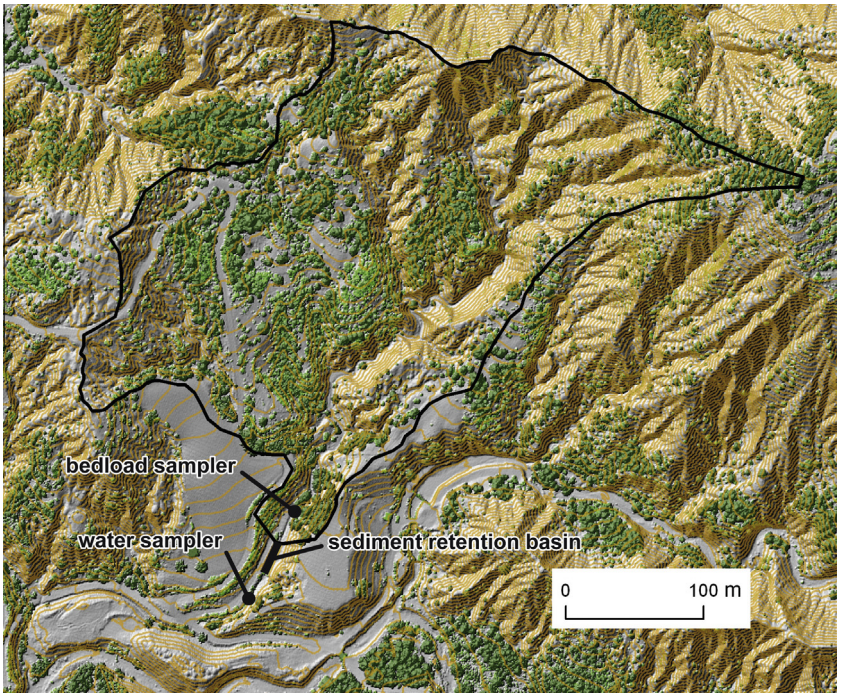

Fig. 1. Hillshade view of the Moulin Ravine catchment derived from a 1 m resolution Digital Elevation Model (2007 airborne LiDAR data); 2 m contour levels in orange, catchment divide in black, and vegetation cover in green. (For interpretation of the references to colour in this figure legend, the reader is referred to the web version of this article.)

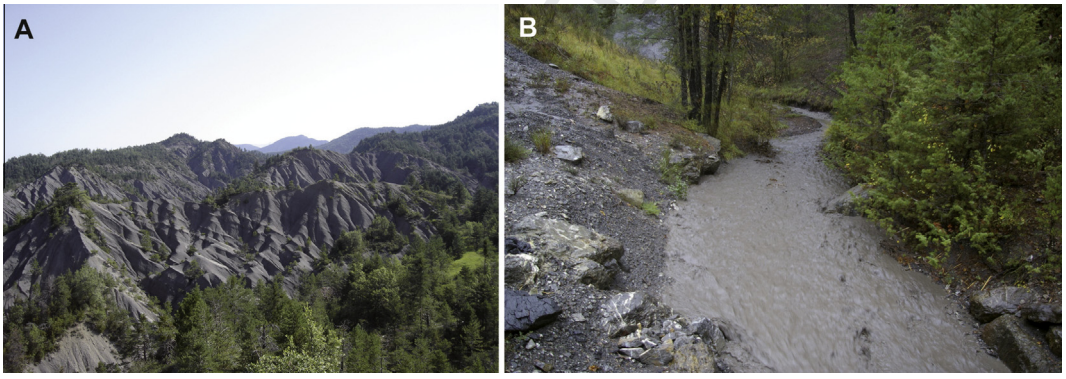

Fig. 2. Typical black marl badlands at Draix (A), and a view from the location of the slot sampler upstream to the Moulin Ravine during a flow event with water discharge ~20 L s^{-1}(B).

to allow viewing the sediment and accordingly to facilitate sediment facies sampling for grain-size distribution (GSD) analysis, and to photograph the bedload deposit before emptying the box (following recommendations by Bergman et al., 2007). The cover plate was designed with a slot of adjustable width and position across the channel (Fig. 3B). The streamwise length of the slot was fixed at 50 cm (more than 100 times the surface D_{50}), which is sufficiently long to trap particles moving in saltation (Laronne et al., 2003). A calibration of the pressure response was undertaken with concrete slabs of known mass to obtain the empirical relation between the *submerged* mass and the pressure difference between the two transducers. This operation confirmed the expected linear response with an empirical constant of 399.9, in agreement with the theoretical constant of 395.8 calculated from the area of contact between the pillow and the inner box, the difference being mainly due to friction of the weighing apparatus (M_{bs} = 399.9 ($\Delta_H - \Delta_{H0}$), r^2 = 0.99, SE = 1.86 kg, with M_{bs}, the *submerged* mass of sediment in kg, Δ_H the pressure difference between the two sensors in cm of water, and Δ_{H0} the pressure difference between the two sensors when the inner box is empty of sediment, in cm of water). The two pressure transducers are connected to a Campbell CR1000 data logger sampling the signal at a frequency of 10 s.

The bedload sampler has been operating continuously in the Moulin Ravine since September 2011. The slot width was initially fixed at 4 cm, representing 20 times the surface D_{50} of the channel. In April 2013, the monitoring procedure was modified by the deployment of small vanes on each side of the slot, and the slot width was enlarged to 8 cm (Fig. 3B). This was justified based on analysis of the first monitored flow events, from which unrealistically high bedload fluxes were obtained by considering a sampling width of 4 cm. This was confirmed by direct observations of the flow pattern in proximity to the sampler during active bedload transport, revealing significant bedload sampling from the streamwise sides of the slot.

Please cite this article in press as: Liébault, F., et al. Bedload monitoring under conditions of ultra-high suspended sediment concentrations. J. Hydrol. (2016), http://dx.doi.org/10.1016/j.jhydrol.2016.07.014

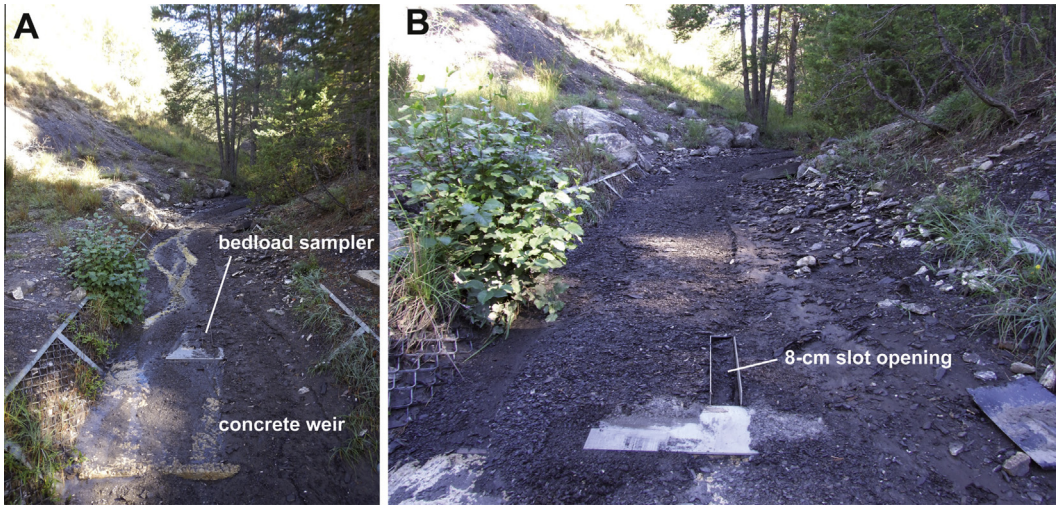

Fig. 3. Views looking upstream of the bedload sampler showing (A) the alluvial approach reach and the concrete weir constructed to stabilize the channel, and (B) the 8 cm slot opening with small lateral vanes to ensure bedload sampling takes place only from the upstream cross-section of the slot.

3.2. Data processing and ancillary data

When the difference of pressure increase during a time increment exceeds the critical level of detection of sediment deposition in the box (dependent on sensor precision), a *submerged* bedload mass is computed using the calibration constant and the difference of pressure when the box is empty of sediment. The conversion to bedload mass is done using a sediment density (ρ_s) of 2650 kg m^{-3}, and a fluid density (ρ) computed from the SSC obtained with the water sampler. The sampler is deployed downstream of the sediment retention basin, in a concrete channel, where it is coupled with a trapezoidal sharp-crested weir for water discharge monitoring (Fig. 1). An attempt to deploy a sampler close to the bedload sampler was unsuccessful due channel instability. The fraction of sediment below 63 μm was routinely removed from the bedload mass, by means of a systematic GSD analysis of sediment deposited in the sampler. Following Powell et al. (2001), 10 cm horizontal slices of sediment were sampled from the side-wall door of the inner box during each cleaning operation. Samples were sieved down to 63 μm, using half-phi size classes above 8 mm, 1-phi classes for the range 2–8 mm, and two classes for the range 0.063–2 mm (using the 0.5 mm sieve). The fraction below 63 μm was obtained by subtracting the dry mass of the sample before and after sieving, the difference corresponding to the mass passing through the 63 μm sieve. The five largest grains of each 10 cm slice were manually extracted and the three axes were measured using a caliper. Bedload flux was calculated by normalizing the bedload mass by the slot width, and the time increment taken at 10 s.

The channel-average shear stress ($\tau = \rho gRs$) associated with 10 s bedload transport rates was computed using the fluid density (ρ) integrating fine sediment concentration, the constant of gravitation (g), the hydraulic radius (R) computed for the cross-section at the sampler, and the slope of the energy gradient (s), which was assumed equal the streambed slope (assumption of steady and uniform flow regime). This is justified by the uniform and controlled geometry of the channel reach where the sampler has been deployed.

4. Results

4.1. Instantaneous bedload transport rates during summer flash flows

The slot sampler enabled collecting a database on instantaneous bedload fluxes in conditions of very high SSC. Four examples of bedload recording during flashy summer flow events are presented (Fig. 4). The June 2013 flow event is the highest recorded since the onset of bedload monitoring. It was triggered by a short duration convective storm. The 1.38 m^3 s^{-1} peak discharge recorded by the Parshall-flume gauging station of the Moulin surpasses the 20-yr recurrence-interval instantaneous peak discharge of the ravine, estimated at 1.3 m^3 s^{-1} (Mathys, 2006). The 60 cm maximum water depth above the sampler occurred 14 min after the onset of flow, illustrating the flashy nature of this flow regime. A mean SSC of 187 g L^{-1} with a maximum value of 319 g L^{-1} were obtained from the six samples collected during the period of effective bedload recording (excluding the period of time when bedload is active but the sampler is full) (Fig. 5A).

Bedload fluxes were computed for 10 s time steps from the cumulative pressure response of the slot sampler. Major segments of this cumulative curve were used to isolate eight successive periods of bedload transport during the event (referred as P1 to P8 in Fig. 4A). During the first three periods bedload response follows fluctuations in water depth. The maximum bedload flux is recorded during P2, with a remarkable value of 37.3 kg m^{-1} s^{-1}. During P4 and P5 bedload response does not mimic hydrograph rise, and bedload fluxes are lower than expected in comparison to prior values (P1–P3). It is very likely that the P4 and P5 bedload recordings were affected by a partial closure of the upstream cross-section of the slot. The 4 cm wide section between the vanes was too short to avoid obstruction by moving coarse particles, and the slot width was enlarged to 8 cm after this event to improve sampling. A coarse grain with a *b*-axes as large as 9.2 cm was, indeed, found in the inner box of the sampler and the mean *b*-axes of the 45 largest grains collected during this event reaches 4.5 cm. The entrance of grains in the sampler is at times controlled by the *c*-axes, explaining why some grains with *b*-axes larger than the slot width were found in the bedload mass. Coarse marl stones of the Moulin are indeed very flat, with a *c*-axes much smaller than the *b*-axes. These observations clearly show that particles larger than the slot opening were mobile during the flow event. This obstruction effect was confirmed by the cessation of bedload recording during the following period (P6), which occurs even though the sampler was only partially filled with sediment: altogether 380 kg relative to a full capacity of 440 kg. The last period of bedload recording occurs during flow recession (P7), likely under the effect of a sudden reopening of the slot. This recording lasted only 1 min and stopped when the trap was full.

Another convective storm took place at the Moulin Ravine in late July 2013 during the night, triggering a flash flow event with

Please cite this article in press as: Liébault, F., et al. Bedload monitoring under conditions of ultra-high suspended sediment concentrations. J. Hydrol. (2016), http://dx.doi.org/10.1016/j.jhydrol.2016.07.014

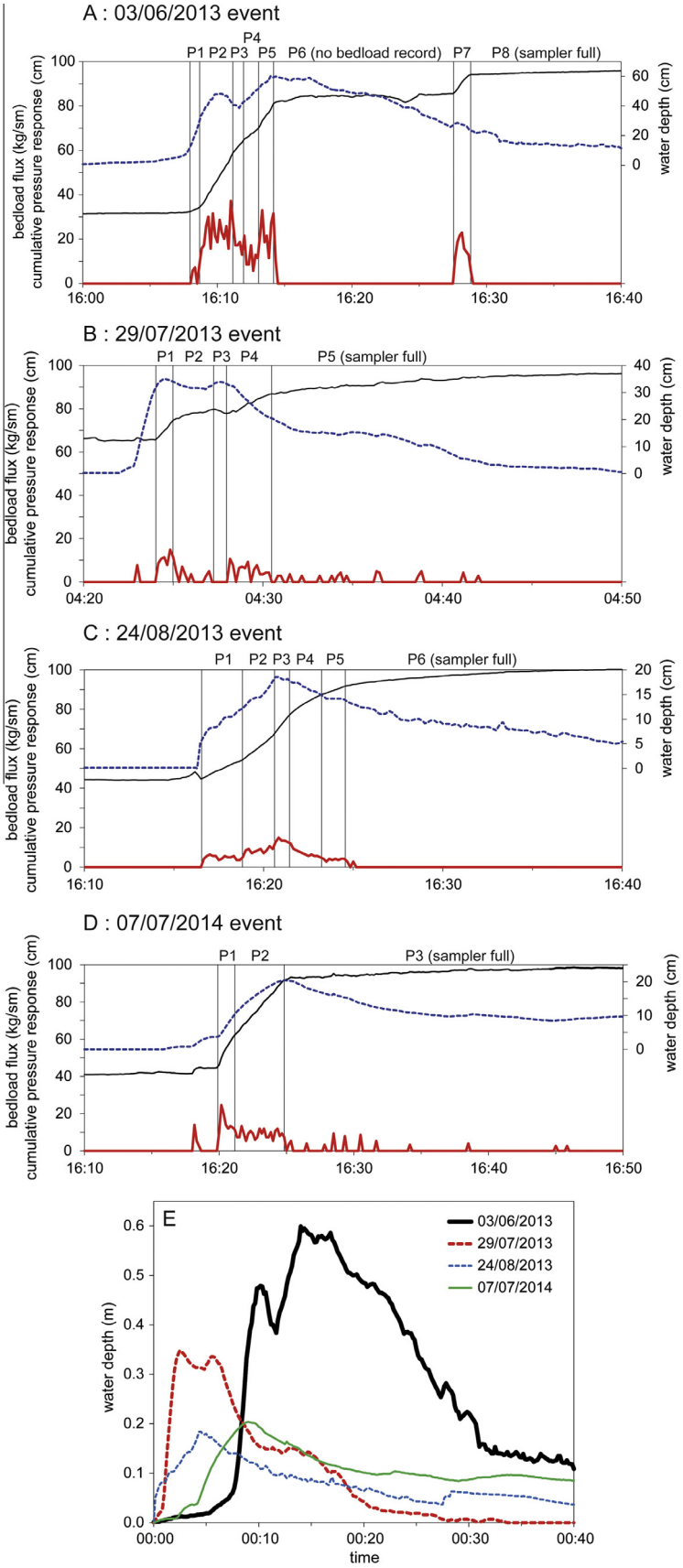

Fig. 4. Stage hydrographs (blue dashed line), cumulative pressure responses (black thin line), and bedload flux (red thick line) observed during four extreme flash flow events in the Moulin Ravine. Periods during which slices of deposited bedload were sampled have been manually determined from breaklines of the pressure response curves (as per Powell et al., 2001; Lucia et al., 2013). The scale of water depth differs between panels. For comparison, hydrographs of the four flow events are presented using the same vertical and horizontal scales in panel E. (For interpretation of the references to colour in this figure legend, the reader is referred to the web version of this article.)

Please cite this article in press as: Liébault, F., et al. Bedload monitoring under conditions of ultra-high suspended sediment concentrations. J. Hydrol. (2016), http://dx.doi.org/10.1016/j.jhydrol.2016.07.014

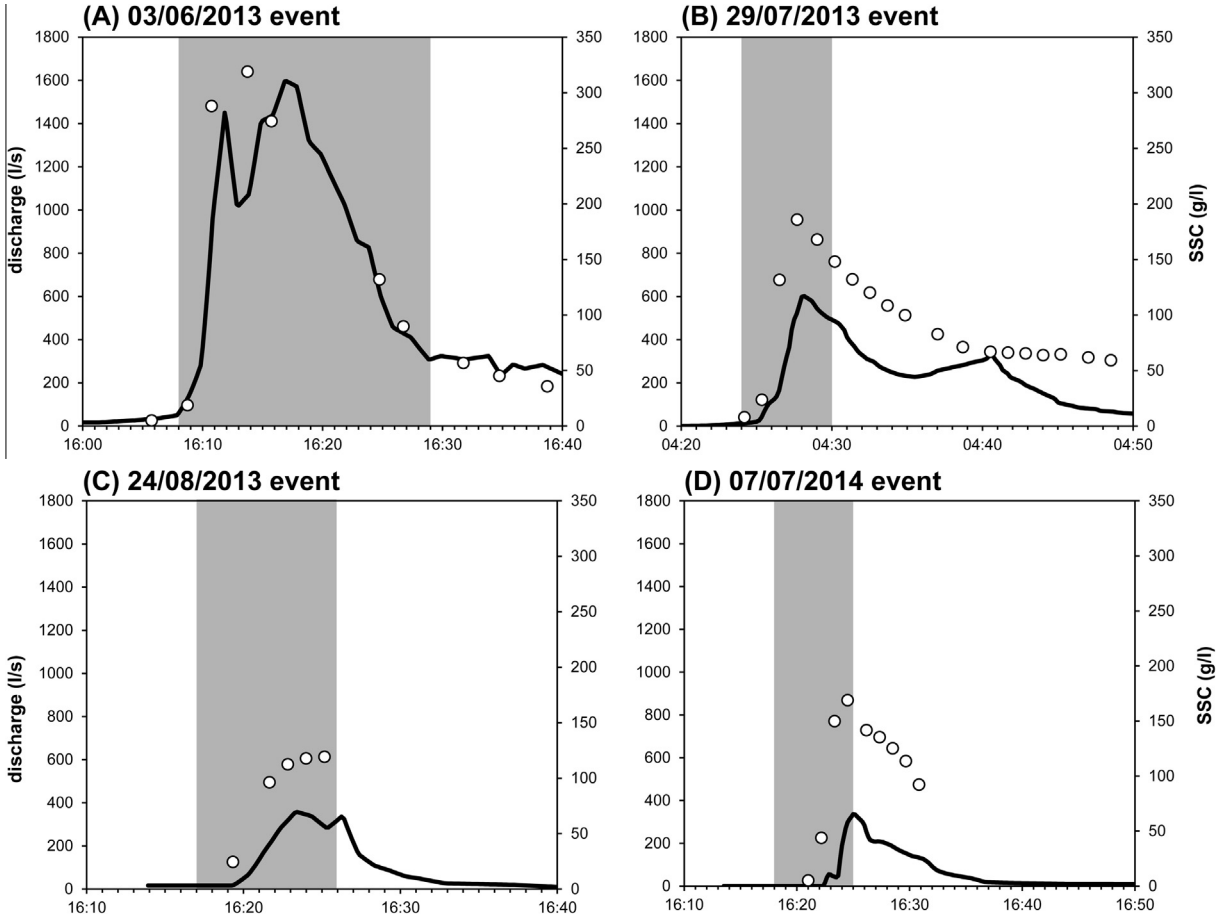

Fig. 5. Suspended sediment concentration obtained from automatic sampling (open symbols) and discharge hydrographs of the four investigated flow events; periods of effective automatic bedload recording are represented by shaded zones.

a peak discharge of 0.60 $m^3 s^{-1}$. A 35 cm peak water depth above the sampler was recorded only 2 min after runoff initiation (Fig. 4B). The water depth lasted as high during four minutes, and a long (25 min) recession followed. A mean SSC of 103 g L^{-1} was obtained from 5 water samples (range: 8–186 g L^{-1}, Fig. 5B). Five periods of similar bedload response were separated. The first period includes the end of the rising stage and the peak of the hydrograph, during which the maximum 10 s bedload flux of 15.0 kg $m^{-1} s^{-1}$ is recorded. The bedload sampling starts late during the rising limb; the first detected bedload mass corresponds to a water depth as high as 33 cm, very close to peak stage. The following two periods (P2 and P3) show a dramatic decrease of bedload transport, with a cessation of transport during P3, whereas these periods correspond to the water depth plateau preceding the recession limb. A partial closure of the slot opening is again suspected here. The presence of a 7.4 cm diameter particle in the inner box during this event again attests that a partial closure of the 8 cm slot opening was a possible outcome. Bedload recording restarts during the recession (P4), until the maximum capacity of the inner box was reached (P5).

One month later, a new bedload record was produced during a late August thunderstorm, which generated a peak discharge of 0.21 $m^3 s^{-1}$. The hydrograph differed from the two previous events (Fig. 4C). A 4 min rise with a single 18 cm peak was immediately followed by a slow recession, without any marked plateau. The 94 g L^{-1} mean SSC obtained from 5 water samples (range: 24–119 g L^{-1}, Fig. 5C) is very close to the value observed during the July 2013 event. Antecedent conditions also differed from the two previous events, for which the slot sampler was full of water before runoff initiation. This is not the case here, where drier conditions explain a low level of water in the sampler before the flow, and the subsequent lack of bedload data at the very beginning of the flow. Six periods of bedload transport were detected, with the first two periods corresponding to the rising limb where a progressive increase of bedload transport was detected. The third period during which the peak flow is observed includes the maximum 10 s bedload flux, reaching a value of 14.9 kg $m^{-1} s^{-1}$, very close to the one observed during the July 2013 event, although the peak of water stage for this event is half that of the previous event. The following two periods (P4 and P5) correspond to the recession, during which bedload transport gradually decreases until the sampler was full (P6). Bedload recording is much less chaotic relative to the previous events. Indeed the smaller size of the largest sampled clast (5.7 cm) relative to the 8 cm slot width supports a free passing of grains through the slot into the sampler during the entire bedload recording period.

The fourth bedload record was collected during early summer 2014. The associated flow event is very similar to the August 2013 event, with a 0.19 $m^3 s^{-1}$ peak water discharge and a typical triangular-shaped hydrograph, with a single 20 cm peak water depth, and a gently sloping recession (Fig. 4D). A mean SSC of 92 g L^{-1} was obtained from four water samples (range: 5–168 g L^{-1}, Fig. 5D). Three periods of bedload response were detected. The first period corresponds to the early and steep rising limb, during which the peak 10 s bedload flux of 24.6 kg $m^{-1} s^{-1}$ was recorded. The second segment is also during the rising stage to peak flow, during which stage increased more slowly than at first. During P2, bedload fluxes fluctuate about 10 kg $m^{-1} s^{-1}$, with

Please cite this article in press as: Liébault, F., et al. Bedload monitoring under conditions of ultra-high suspended sediment concentrations. J. Hydrol. (2016), http://dx.doi.org/10.1016/j.jhydrol.2016.07.014

a gradual increase of bedload flux with increase in water depth. The full capacity of the sampler was attained during peak flow. The largest recovered bedload particle (5.6 cm) indicates that slot obstruction was unlikely. This is supported by the pattern of bedload responding to flow depth, less so chaotic than for the June and July 2013 events.

4.2. Grain-size distributions of bedload samples

The integrated GSD of sediment collected in the sampler during each flow event was determined by grouping all slices attributed to a given event into a composite sample. The combination of elementary size classes above 0.063 mm into 5 groups provides a synthetic representation of the GSD (Fig. 6A). These groups correspond to very fine, fine and medium sands (0.063–0.5 mm), coarse and very coarse sands (0.5–2 mm), very fine and fine pebbles (2–8 mm), medium and coarse pebbles (8–32 mm), and very coarse pebbles (32–45 mm). The full GSDs using cumulative curves are also presented (Fig. 6B). The emerging pattern from composite samples reveals a contrasting bedload GSD between the June 2013 flow event and the other events. A prevalence of medium and coarse pebbles is observed during the June 2013 event, whereas very fine and fine pebbles dominate in the three other events. The June 2013 event is also characterized by the appearance of very coarse pebbles, and a simultaneous decreasing proportion of coarse and very coarse sands. The coarsening of the bedload GSD during this event is in agreement with its much higher peak discharge, 2–7 times larger than that of the following events. If the fraction above 0.5 mm is considered to be representative of the transported bedload, summary parameters derived from truncated GSDs clearly document bedload coarsening with increasing peak discharge (Table 1). The sevenfold increase in discharge covered by observations shifted the bedload GSD from a fine-pebble dominated distribution with $D_{50} \sim 4$–5 mm ($D_{90} \sim 12$–13 mm), to a coarse-pebble dominated distribution with $D_{50} \sim 8$ mm ($D_{90} \sim 25$ mm).

Silts and clays represent between 15 and 23% of the distribution (see F_f values reported in Fig. 6), indicating that the deposited mass cannot be entirely attributed to bedload transport. This proportion of fine-grained sediments deposited in the sampler (F_f) does not show any covariation with flow magnitude. This is also true for the fraction between 0.063 and 0.5 mm. One could intuitively expect a decreasing proportion of fines in the sampler with increasing discharge, but another critical factor independent of hydraulics must explain the amount of trapped fines (see Section 5.1). If the fraction above 0.5 mm is considered, assuming that the medium sand class is likely to represent the transition between bedload and suspended load, it appears that bedload encompasses between 71 and 79% of the mass.

The presence of silts and clays inside the sampler indicates that a fraction of the suspended load is captured by the sampler during bedload transport. How important is this fraction with respect to the total suspended sediment mass passing through the slot width during bedload recording? This has been assessed by comparing the mass of fines deposited in the sampler with the mass of fines transported through the slot width, estimated using water discharge and SSC data (Fig. 5). The amount of fines entering the sampler as a fraction of the SSL is always below 10%, and it decreases from ca. 10% to 1% with increase in water discharge (Table 2).

Inspection of the vertical variability of fines inside the sampler provides information about the intra-event variability of the content of fine (Fig. 7). Although one event shows a classic pattern of fine enrichment in the uppermost layers (August 2013 event), others are characterized by a fairly stable 15% fraction of fines (July 2013 event), or by enrichment of fines in the bottom and the top layers (June 2013 and July 2014 events).

The intra-event variability of fines can be taken in consideration for the computation of instantaneous bedload flux following the approach of Powell et al. (2001), provided that each bedload layer can be easily redistributed in time. This is not straightforward for

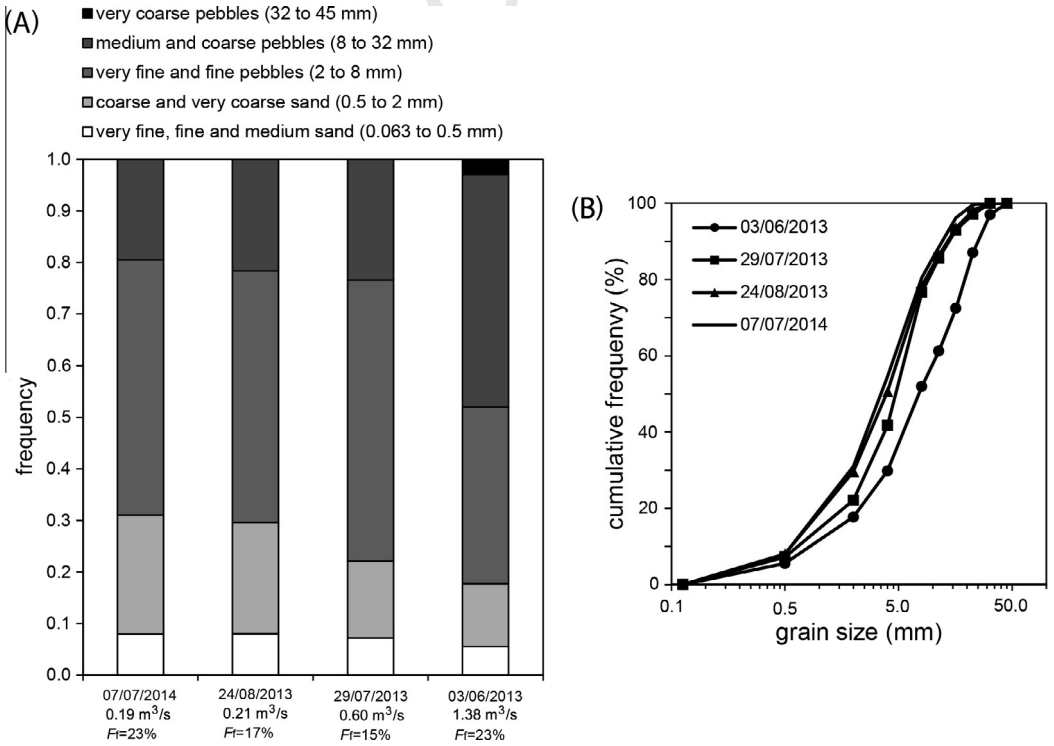

Fig. 6. (A) Proportions of sand and pebbles collected in the slot sampler during four summer flow events; discharge values refer to the peak discharge of each event; F_f is the proportion of fines (silts and clays) deposited in the sampler. (B) Cumulative curves of lower 0.063 mm truncated GSDs for each flow event.

Please cite this article in press as: Liébault, F., et al. Bedload monitoring under conditions of ultra-high suspended sediment concentrations. J. Hydrol. (2016), http://dx.doi.org/10.1016/j.jhydrol.2016.07.014

Table 1
Summary parameters of the composite bedload grain-size distributions obtained for each flow with a lower 0.5 mm truncation.

Flow events	03/06/2013	29/07/2013	24/08/2013	07/07/2014
D_{16} (mm)	2.4	2.0	1.6	1.6
D_{50} (mm)	8.2	5.1	4.4	3.9
D_{84} (mm)	21.5	11.1	10.8	9.8
Coarse and very coarse sands, 0.5–2 mm (%)	13	16	23	25
Very fine and fine pebbles, 2–8 mm (%)	36	59	53	54
Medium and coarse pebbles, 8–32 mm (%)	48	25	23	21
Very coarse pebbles, 32–64 mm (%)	3	0	0	0

Table 2
Evaluation of the fraction of the suspended sediment load trapped in the bedload sampler during flow events.

Flow events	03/06/2013	29/07/2013	24/08/2013	07/07/2014
Suspended sediment load, SSL (kg)[a]	7874	2408	969	837
Silts and clays deposited in the sampler (%)	22.6	15.1	16.8	22.6
Silts and clays deposited in the sampler (kg)	105	32	55	78
Fraction of the SSL trapped in the sampler (%)	1.3	1.3	5.7	9.3

[a] Total SSL transported over the slot width during the flow.

the Moulin, as the bulk sediment density changes with the amount of fines, implying additional analysis for unequivocal time redistribution of sediment layers. Another difficulty to consider in this respect is the extent to which stratigraphy of bedload layers are visible from the side-wall door; indeed this is not easy to interpret given the dark hue of the sedimentary particles. We did detect a steep (~20°) downstream sloping dip of the bedload layers (Fig. 8), which indicates that sampling sediment through the door may miss the first deposited layers. The ideal method of sampling would be to adopt an event-specific protocol constrained by stratification, while being careful to collect the same distal position for each layer, as it is also recognized that the GSD fluctuates with the distance to the upstream edge of the slot (Habersack et al., 2001).

4.3. Bedload response to shear stress

The bedload response to shear stress was investigated by plotting 10 s and 60 s bedload flux as a function of shear stress (Fig. 9A and B). In these diagrams bedload flux is presented in a nondimensional form ($I_b^* = (I_b/\rho_s)[gD_{50}^3(\rho_s - \rho)/\rho]^{0.5}$), and shear stress is expressed by the Shields number ($\tau^* = \tau/gD_{50}(\rho_s - \rho)$) using the bedload D_{50} and the total shear stress. The periods during which bedload sampling is considered to be unbiased appear in colors. As previously explained in the presentation of coincident variations of bedload flux and flow stage, some sampling periods were affected by a decreasing sampling efficiency when the sampler was full or almost full of sediment (P5 of the July 2013 event and P7 of the July 2014 event). This is in agreement with previous findings (Habersack et al., 1998) documenting a significant increase of flow velocity inside the sampler at 80% fill. The P1 period of the July 2014 event was also excluded since the very high bedload fluxes recorded here were likely explained by the deposition of a mud bore, as attested by the unusually high proportion (39%) of fines (<0.5 mm) in the first layer deposited in the sampler during this event. This is confirmed by the unrealistic values of the dimensionless bedload fluxes recorded for this period, plotting one order of magnitude higher than the highest hitherto reported values in the field for equivalent Shields numbers (Fig. 9B). Other peri-

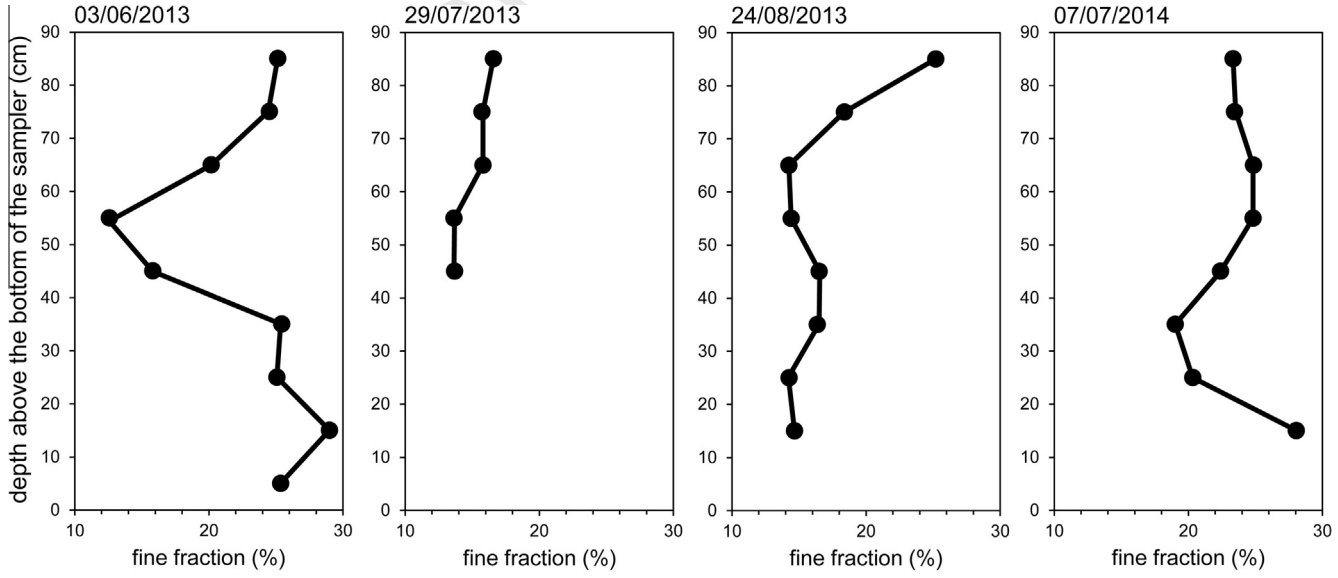

Fig. 7. Vertical variability of the fine fraction (<0.063 mm) during four summer flow events; each point corresponds to a 10 cm thick slice taken from the side-wall door of the bedload sampler.

Please cite this article in press as: Liébault, F., et al. Bedload monitoring under conditions of ultra-high suspended sediment concentrations. J. Hydrol. (2016), http://dx.doi.org/10.1016/j.jhydrol.2016.07.014

Fig. 8. Photograph of bedload layers visible through the side-wall door of the sampler, showing a ~20° downstream sloping (dashed white lines) deposit.

ods were likely affected by partial or total closure of the slot opening by coarse particles (P4-5-6 of the June 2013 event, P2-3 of the July 2013 event). This is supported by the presence of grains with *b*-axes similar to and even larger than the slot width in the collected bedload mass, but alternative explanations cannot be excluded, such as a lateral shift of the flow during the event or a dramatic sediment supply decrease during the event under the effect of bedload sheet migration. However, the lack of evidence supporting these alternative explanations make them more speculative.

Bedload fluxes show simple linear increases with shear stress, as attested by linear regressions to the data providing good fits (Fig. 9A). It has been possible to fit linear regressions only by considering each event independently (Fig. 9A). It was not possible to obtain a good fit for the July 2014 event, but for the three others highly significant trends were obtained ($p < 0.0001$), with $0.36 < r^2 < 0.66$. If periods during which a partial or total closure of the slot is expected are included, a significant linear fit is conserved for the July 2013 event ($r^2 = 0.26$, $p = 0.0103$), but not for the June 2013 event. The linear fits for the events of June and August 2013 reveal very similar bedload responses, whereas a different behavior is observed in July 2013. Although the slope of the July 2013 linear fit is not statistically different from the two others (at a 5% risk of error), its intercept is much higher. Data for this event are shifted toward high shear stress values, indicating much less efficient bedload transport, and a much higher incipient motion. The critical dimensionless shear stress can be estimated with the linear fits, by considering the minimum 10 s bedload flux that can be detected by the sampler. This computation gives values of 0.28, 0.77, and 0.37, for the June, July, and August 2013 events,

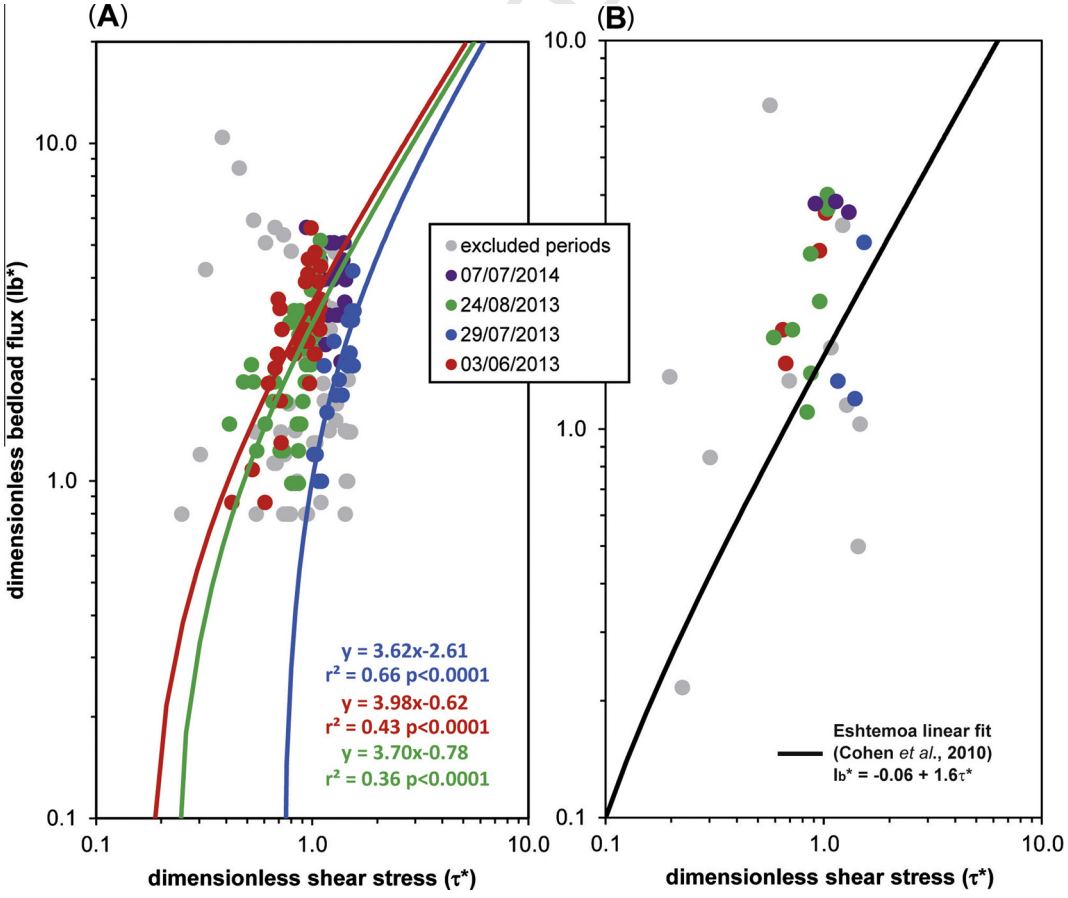

Fig. 9. Bedload response to shear stress during four summer flow events at the Moulin Ravine; bedload fluxes were computed for time steps of 10 s (A) and 60 s (B).

Please cite this article in press as: Liébault, F., et al. Bedload monitoring under conditions of ultra-high suspended sediment concentrations. J. Hydrol. (2016), http://dx.doi.org/10.1016/j.jhydrol.2016.07.014

respectively. It was not possible to propose a value for the June 2014 event, but the position of points obtained for this event in Fig. 9A suggests an intermediate bedload response.

Bedload fluxes at 60 s time steps were computed to provide a comparison with a reference dataset of very high bedload transport collected on the Nahal Eshtemoa in Israel (Cohen et al., 2010), from which a linear bedload response to shear stress was obtained using a 60 s sampling interval. This dataset was used because it is considered to be representative of bedload response to flow in unlimited sediment supply conditions (e.g., Hayes et al., 2002). Data points from the Moulin are clearly positioned close to the Eshtemoa linear fit, although most of them are above the trend (Fig. 9B). It is, however, difficult to conclude about a higher bedload regime of the Moulin, given the small number of bedload records used in this study. This analysis mainly reveals that the bedload response of the Moulin is similar to the one observed in the Eshtemoa.

5. Discussion

5.1. Sensitivity of the automatic bedload sampler to fines under ultra-high SSC

The continuous bedload monitoring of the Moulin Ravine allows testing for the first time a Reid-type slot sampler under conditions of ultra-high SSC. Early laboratory experiments (Poreh et al., 1970) demonstrated that slot samplers are insensitive to fine particles, but this technique had never been tested in channels transporting such a high suspended sediment concentration as does the Moulin. The only examples with sediment transport conditions close to Draix are the arid and semi-arid fluvial settings in Israel (e.g. Reid et al., 1995; Cohen and Laronne, 2005; Alexandrov et al., 2009), where usual SSCs during bedload records are on average 40 g L^{-1}. Maximum SSCs measured in the Moulin during this study are in the range 120–320 g L^{-1}.

The GSD analysis of trapped sediments reveals that silts and clays enter the sampler during bedload transport. This fine fraction, which represents 15–23% of the deposited mass, demonstrates that part of the suspended load enters the slot and that the deposited mass cannot be entirely attributed to bedload. This estimate of the SSL fraction in the sampler can be even larger if one considers a suspension criteria based on the settling velocity of grains using explicit equations (Dietrich, 1982; Ferguson and Church, 2004). The shear velocities ($u^* = (\tau/\rho)^{0.5}$) were used to determine the grain size below which particles should be transported in suspension, according to the settling velocity approach. The two analytical expressions of the settling velocity show that grains as large as 6–8 mm should be transported in suspension for the flow conditions observed in the Moulin (range: 2.7–8.6 mm). If this is assumed, more than 50% (range: 48–67%) of the mass in the sampler derives from the SSL. This is quite unrealistic, and physically impossible (Poreh et al., 1970). Slots samplers are considered to be the most efficient device separating bedload from the suspended load both under flume conditions and in the field. Unfortunately, we did not obtain data on the GSD of the Moulin SSL; nonetheless such data are available for the Laval, a 1 km^2 experimental catchment of Draix draining the same geological formation. The D_{90} of the SSL during a flashy summer flow event was in the range 0.018–0.086 mm for water discharges between 10 and 6000 L s^{-1} (Mathys, 2006). Sands represented only 1–15% of the SSL. These previous observations support our interpretation of the results from settling velocities. Even if it has not been possible to constrain the size of sediments transported in suspension in the Moulin, previous investigations in the Laval are in good agreement with the practical separation between bedload and suspension adopted here.

The comparison of the quantity of fines inside the sampler with the suspended load that transits over the slot width during bedload sampling reveals that fines deposited in the sampler represent only a small fraction of the suspended load (between 1 and 10%), and that this fraction increases inversely with increase in water discharge. During small events SSC is still very high but water velocity is low, thus more time is available for some, still a small percentage, of suspended particles to enter the slot. Indeed the fraction of fines in the sampler does not fluctuate much between events with contrasted flow magnitudes. One possible interpretation is to consider that given the very high content of fines in the bed of the Moulin, bedload particles inevitably carry with them some fines that are embedded in the moving bedload sheets and deposited in the sampler at a proportion equivalent to or somewhat lower than that in the bedload active layer.

Preliminary investigations of the sedimentary composition of the active layer confirmed this interpretation. During summer 2015, a set of 18 sediment samples were collected in the main channel of the Moulin after two flow events for which the bedload active layer was identified using scour chains. Sediment samples were systematically taken from the layer above the scour chain elbow and can, therefore, be attributed to the moving bedload sheet of the last flow event. Analysis of the GSD using the same protocol as for the slot sampler provided the content of fines incorporated in the active layer. This fine fraction varies in the range 13–21% (Fig. 10), in agreement with fluctuations observed in the slot sampler. These data also reveal that for a same position along the channel, the proportion of fines in the active layer from one flow event to another fluctuates between 13% and 20%. This is compatible with a likely critical role of the sedimentary character of the active layer to the fraction of fines trapped in the sampler. A systematic analysis of the composition of the active layer during flow events is required to confirm this interpretation.

A practical implication of the presence of fines in the sampler is the crucial importance to integrate results from the GSD analysis into the computation of bedload flux, thereby avoiding overestimation of bedload transport. This correction has been made by considering the mean proportion of the fine fraction measured for the entire deposited mass during each event, considering that the intra-event variability is not very high. Inspection of the vertical variability of fines inside the sampler reveals that this is true for the July 2013 event, but not for the others where fine enrichment is observed in the bottom and/or top layers. Fine enrichment in the uppermost layers has been explained by secondary flow appearance in the sampler when it is almost full (80%) of sediment (Habersack et al., 2001). The increasing amount of fines in the bottom layers is likely the consequence of the antecedent conditions

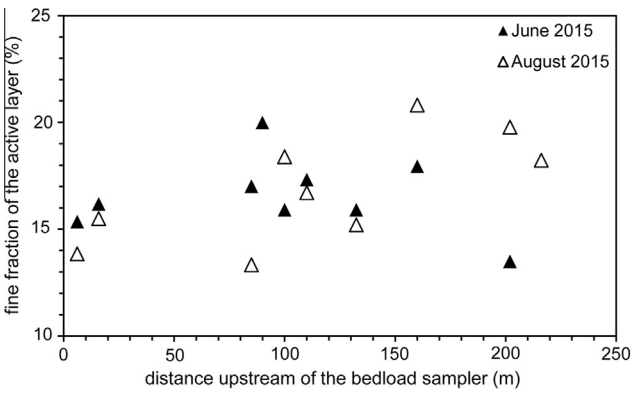

Fig. 10. Proportion of the fine fraction (<0.063 mm) in the active bedload layer along the main channel of the Moulin Ravine sampled after two summer 2015 flow events.

Please cite this article in press as: Liébault, F., et al. Bedload monitoring under conditions of ultra-high suspended sediment concentrations. J. Hydrol. (2016), http://dx.doi.org/10.1016/j.jhydrol.2016.07.014

of the bed when flow starts. During summer, it is common to observe a surficial thin and discontinuous layer of mud in the bed, but the presence of a mud layer is contingent as it depends on the recent flow history.

5.2. Bedload transport responses of marly badlands at Draix

Bedload fluxes in the Moulin integrated over 10 s during summer flow events commonly exceed 10 kg m^{-1} s^{-1}, with a maximum recorded magnitude of 37 kg m^{-1} s^{-1}. These values are equivalent to the highest hitherto reported worldwide, like those in desert streams of Israel (e.g. Laronne and Reid, 1993; Cohen and Laronne, 2005) or in streams impacted by volcanic eruptions (Pitlick, 1992; Hayes et al., 2002). The exceptional bedload transport rate of the Moulin reflects very high sediment supply conditions of unvegetated marly badlands, where active degraded hillslopes are tightly coupled with the stream network. During convective storm-induced summer flow events, coarse sediments can be supplied (i) by channel scouring, even though the commonly observed channel response during summer is aggradation (Mathys, 2006), and (ii) by a direct contribution from hillslopes, under the effect of high intensity rainfall bursts likely to trigger shallow landslides and small debris flows on talus slopes (Oostwoud Wijdenes and Ergenzinger, 1998; Yamakoshi et al., 2009). Another key sediment recharge process revealed by field observations after convective storms is the lateral erosion of dry ravel deposits draping foot slopes at the end of winter. All these complementary sediment sources imply an unlimited sediment supply regime for the Moulin.

The bedload response to shear stress of the Moulin confirms the simple linear response reported for unlimited sediment supply conditions, like in the unarmored Eshtemoa (Cohen et al., 2010). However, contrasted bedload responses are observed between events in the Moulin and the subsequent high data scatter precludes fitting one single curve for the entire dataset. This is likely the consequence of rapidly changing channel conditions of the Moulin alluvial system. This is not only the result of the proximity to sediment sources from hillslopes, which are known to produce seasonal pulses of sediment recharge (Mathys, 2006), but also a consequence of the hydrological contingency, as likely illustrated by the specific response of the July 2013 event. The shifting of its bedload response toward the high shear stress domain likely reflects specific channel conditions associated with the very high flow event of June 2013. Although it has not been possible to document inter-event channel changes, a coarsening of the channel texture has been observed in the Moulin after the June 2013 event, due to the formation of bars with coarse to very coarse pebble-sized grains. This is in agreement with the increase in entrainment threshold of the July 2013 event. The specific bedload response of the July 2013 event can also be attributed to a low sediment supply from hillslopes, most of the easily available loose debris having been likely remobilized during the heavy storm of June 2013. This is supported by the coarse-grained nature of the sediment deposits measured during summer 2013 in the sediment retention basin of the Roubine, a 0.13 ha catchment of the Draix observatory, used to monitor erosion from elementary hillslopes of marly badlands. Storm events associated with the June, July and August 2013 flow events of the Moulin produced 5.29, 1.07, and 0.52 m^3 of coarse sediments at the Roubine, respectively. A systematic analysis of in-channel and hillslope sediment sources affecting bedload responses is another important topic which needs to be specifically addressed using the Moulin bedload record.

It is shown that the dimensionless critical shear stress of the Moulin is one order of magnitude higher than commonly reported values for gravel-bed rivers (e.g. Buffington and Montgomery, 1997). This specific behavior is likely explained by the cohesion and adhesion effects of fines which are largely present in the channel surface and subsurface and which may retard the onset of bedload transport. It is indeed recognized that the intrusion of fines into gravel-bed rivers interstices can increase the critical shear stress by a factor of 2 (Barzilai et al., 2013). Flume experiments also demonstrated an increase of the erosion threshold of fine sandy beds (Panagiotopoulos et al., 1997) or gravels (Perret et al., 2015) under the effect of fine intrusion in the sediment mixture. Moreover, channel clogging by silts and clays is partly controlled by the SSC near the bed (Einstein, 1968). The entirety of these relevant studies provides a possible explanation of the very high entrainment threshold in the Moulin, although this needs to be confirmed by specific experiments using sediment mixtures typical of Draix.

6. Conclusion

The continuous monitoring of bedload in the Moulin Ravine shows that the Reid-type slot sampler performs well under conditions of ultra-high SSC. Results obtained during four convective summer flow events with maximum SSC in the range 120–320 g L^{-1}, including a 20-yr return period flash flood, can be summarized in four main conclusions:

(1) A flow-invariant proportion (ca 15–20%) of silt- and clay-sized grains was captured in the slot sampler. This fine fraction, which is embedded in the bedload active layer in the same proportion, and which represents a minor fraction (1–10%) of the SSL passing through the slot width, likely enters the sampler as moving bedload sheets.
(2) Instantaneous bedload fluxes recorded in the Moulin are amongst the highest hitherto reported values in the world, providing evidence of the exceptional sediment transport conditions of marly Mediterranean badlands of the Southern French Alps.
(3) The dimensionless entrainment threshold for bedload transport of the Moulin is one order of magnitude higher than commonly reported values for gravel-bed rivers. This is interpreted as the cohesion effect induced by the considerable quantity of clays and silts intruded in the channel sediment mixture of the Moulin.
(4) The bedload record for the Moulin confirms the linear bedload response to shear stress in conditions of unlimited sediment supply, even though contrasting bedload responses are observed between flow events, likely under the effect of rapidly changing channel conditions.

Acknowledgements

The bedload monitoring program of the Moulin Ravine was supported by ORE Draix-Bléone, OSUG, and the SedAlp project (European Territorial Cooperation Alpine Space Programme 2007–2013). Thanks to LTHE (UMR5564) and Université Grenoble Alpes (formerly Université Joseph Fourier Grenoble) for hosting JBL during 2010. The authors thank the support by Thomas Gagneux, Julie Favario, Robin Paya and Thomas Bédécarrats for post-event field and laboratory help, Xavier Ravanat and Fred Ousset for the construction and deployment of the slot sampler. Ana Lucia Vela, Philippe Belleudy and Nicolle Mathys are acknowledged for discussions and advice regarding the design and deployment of the slot sampler. This paper benefitted from comments made by two anonymous reviewers and from the editor Tim R. McVicar.

References

Alexandrov, Y., Laronne, J.B., Reid, I., 2007. Intra-event and inter-seasonal behaviour of suspended sediment in flash floods of the semi-arid northern Negev, Israel. Geomorphology 85 (1–2), 85–97. http://dx.doi.org/10.1016/j.geomorph.2006.03.013.

Alexandrov, Y., Cohen, H., Laronne, J.B., Reid, I., 2009. Total water-borne material losses from a semi-arid drainage basin: a 15-year study of the dynamics of suspended, dissolved and bed loads. Water Resour. Res. 45, W08408. http://dx.doi.org/10.1029/2008WR007314.

Antoine, P., Giraud, A., Meunier, M., Van Asch, T., 1995. Geological and geotechnical properties of the "Terres Noires" in southeastern France: weathering, erosion, solid transport and instability. Eng. Geol. 40, 223–234. http://dx.doi.org/10.1016/0013-7952(95)00053-4.

Barzilai, R., Laronne, J.B., Reid, I., 2013. Effect of changes in fine-grained matrix on bedload sediment transport in a gravel-bed river. Earth Surf. Proc. Land. 38 (5), 441–448. http://dx.doi.org/10.1002/esp.3288.

Bergman, N., Laronne, J.B., Reid, I., 2007. Benefits of design modifications to the Birkbeck bedload sampler illustrated by flash-floods in an ephemeral gravel-bed channel. Earth Surf. Proc. Land. 32 (2), 317–328. http://dx.doi.org/10.1002/esp.1453.

Buffington, J.M., Montgomery, D.R., 1997. A systematic analysis of eight decades of incipient motion studies, with special reference to gravel-bedded rivers. Water Resour. Res. 33 (8), 1993–2029. http://dx.doi.org/10.1029/96WR03190.

Cohen, H., Laronne, J.B., 2005. High rates of sediment transport by flashfloods in the Southern Judean Desert, Israel. Hydrol. Process. 19 (8), 1687–1702. http://dx.doi.org/10.1002/hyp.5630.

Cohen, H., Laronne, J.B., Reid, I., 2010. Simplicity and complexity of bed load response during flash floods in a gravel bed ephemeral river: a 10 year field study. Water Resour. Res. 46, W11542. http://dx.doi.org/10.1029/2010WR009160.

Descroix, L., Mathys, N., 2003. Processes, spatio-temporal factors and measurements of current erosion in the French Southern Alps: a review. Earth Surf. Proc. Land. 28, 993–1011. http://dx.doi.org/10.1002/esp.514.

Dietrich, W.E., 1982. Settling velocity of natural particles. Water Resour. Res. 18 (6), 1615–1626. http://dx.doi.org/10.1029/WR018i006p01615.

Einstein, H.A., 1968. Deposition of suspended particles in a gravel bed. J. Hydraul. Eng. 94 (5), 1197–1205.

Ferguson, R.I., Church, M., 2004. A simple universal equation for grain settling velocity. J. Sediment. Res. 74, 933–937. http://dx.doi.org/10.1306/051204740933.

Gao, G., Ma, Y., Fu, B., 2015. Temporal variations of flow–sediment relationships in a highly erodible catchment of the Loess Plateau, China. Land Degrad. Dev. http://dx.doi.org/10.1002/ldr.2455.

Garcia, C., Laronne, J.B., Sala, M., 2000. Continuous monitoring of bedload flux in a mountain gravel-bed river. Geomorphology 34, 23–31. http://dx.doi.org/10.1016/S0169-555X(99)00128-2.

Garcia-Ruiz, J.M., Regüés, D., Alvera, B., Lana-Renault, N., Serrano-Muela, P., Nadal-Romero, E., Navas, A., Latron, J., Marti-Bono, C., Arnáez, J., 2008. Flood generation and sediment transport in experimental catchments affected by land use changes in the central Pyrenees. J. Hydrol. 356 (1–2), 245–260. http://dx.doi.org/10.1016/j.jhydrol.2008.04.013.

Gerson, R., 1977. Sediment transport for desert watersheds in erodible materials. Earth Surface Process. 2 (4), 343–361. http://dx.doi.org/10.1002/esp.3290020407.

Habersack, H.M., Nachtnebel, H.P., Laronne, J.B., 1998. The hydraulic efficiency of a slot sampler: flow velocity measurements in the Drau River, Austria. In: Klingeman, P., Beschta, R., Komar, P., Bradley, B. (Eds.), Gravel-Bed Rivers in the Environment. Water Resources Publications, LLC, Highlands Ranch, Colorado, pp. 749–754.

Habersack, H.M., Nachtnebel, H.P., Laronne, J.B., 2001. The continuous measurement of bedload discharge in a large alpine gravel bed river. J. Hydraul. Res. 39 (2), 125–133. http://dx.doi.org/10.1080/00221680109499813.

Hayes, S.K., Montgomery, D.R., Newhall, C.G., 2002. Fluvial sediment transport and deposition following the 1991 eruption of Mount Pinatubo. Geomorphology 45, 211–224. http://dx.doi.org/10.1016/S0169-555X(01)00155-6.

Laronne, J.B., Reid, I., 1993. Very high rates of bedload sediment transport by ephemeral desert rivers. Nature 366 (6451), 148–150. http://dx.doi.org/10.1038/366148a0.

Laronne, J.B., Alexandrov, Y., Bergman, N., Cohen, H., Garcia, C., Habersack, H., Powell, D.M., Reid, I., 2003. The continuous monitoring of bedload flux in various fluvial environments. In: Bogen, J., Fergus, T., Walling, D.E. (Eds.), Erosion and Sediment Transport Measurement in Rivers: Technological and Methodological Advances, vol. 283. International Association of Hydrological Sciences Publication, pp. 134–145.

Lucia, A., Recking, A., Martin-Duque, J.F., Storz-Peretz, Y., Laronne, J.B., 2013. Continuous monitoring of bedload discharge in a small, steep sandy channel. J. Hydrol. 497, 37–50. http://dx.doi.org/10.1016/j.jhydrol.2013.05.034.

Mathys, N., 2006. Analyse et modélisation à différentes échelles des mécanismes d'érosion et de transport de matériaux solides: cas des petits bassins versants de montagne sur marne (Draix, Alpes-de-Haute-Provence) Unpublished PhD Thesis. Institut National Polytechnique de Grenoble, p. 306.

Mathys, N., Brochot, S., Meunier, M., Richard, D., 2003. Erosion quantification in the small marly experimental catchments of Draix (Alpes de Haute Provence, France), calibration of the ETC rainfall-runoff-erosion model. Catena 50 (2–4), 527–548. http://dx.doi.org/10.1016/S0341-8162(02)00122-4.

Mizuyama, T., Laronne, J.B., Nonaka, M., Sawada, T., Satofuka, Y., Matsuoka, M., Yamashita, S., Sako, Y., Tamaki, S., Watari, M., Yamaguchi, S., Tsuruta, K., 2010. Calibration of a passive acoustic bedload monitoring system in Japanese mountain rivers. In: Gray, J.R., Laronne, J.B., Marr, J.D.G. (Eds.), Bedload-surrogate Monitoring Technologies. U.S. Geological Survey Scientific Investigations Report 2010-5091, pp. 296–318.

Nadal-Romero, E., Martinez-Murillo, J.F., Vanmaercke, M., Poesen, J., 2011. Scale-dependency of sediment yield from badland areas in Mediterranean environments. Prog. Phys. Geogr. 35 (3), 297–332. http://dx.doi.org/10.1177/0309133311400330.

Navratil, O., Evrard, O., Esteves, M., Legout, C., Ayrault, S., Némery, J., Mate-Marin, A., Ahmadi, M., Lefèvre, I., Poirel, A., Bonté, P., 2012. Temporal variability of suspended sediment sources in an alpine catchment combining river/rainfall monitoring and sediment fingerprinting. Earth Surf. Proc. Land. 37, 828–846. http://dx.doi.org/10.1002/esp.3201.

Oostwoud Wijdenes, D.J., Ergenzinger, P., 1998. Erosion and sediment transport on steep marly hillslopes, Draix, Haute-Provence, France: an experimental field study. Catena 33, 179–200. http://dx.doi.org/10.1016/S0341-8162(98)00076-9.

Owens, P.N., Batalla, R.J., Collins, A.J., Gomez, B., Hicks, D.M., Horowitz, A.J., 2005. Fine-grained sediment in river systems: environmental significance and management issues. River Res. Appl. 21 (7), 693–717. http://dx.doi.org/10.1002/rra.878.

Panagiotopoulos, I., Voulgaris, G., Collins, M.B., 1997. The influence of clay on the threshold of movement of fine sandy beds. Coast. Eng. 32 (1), 19–43. http://dx.doi.org/10.1016/S0378-3839(97)00013-6.

Perret, E., Herrero, A., Berni, C., Abderrezzak, K.E.K., Camenen, B., 2015. Incipient motion of a bimodal mixture of gravel and silt: a laboratory experimental study. In: E-Proceedings of the 36th IAHR World Congress. The Hague, Netherlands, p. 11.

Pitlick, J., 1992. Flow resistance under conditions of intense gravel transport. Water Resour. Res. 28 (3), 891–903. http://dx.doi.org/10.1029/91WR02932.

Poreh, M., Sagiv, A., Seginer, I., 1970. Sediment sampling efficiency of slots. J. Hydraul. Div. 96 (10), 2065–2078.

Powell, D.M., Reid, I., Laronne, J.B., 2001. Evolution of bed load grain size distribution with increasing flow strength and the effect of flow duration on the caliber of bed load sediment yield in ephemeral gravel bed rivers. Water Resour. Res. 37 (5), 1463–1474. http://dx.doi.org/10.1029/2000WR900342.

Reid, I., Layman, J.T., Frostick, L.E., 1980. The continuous measurement of bedload discharge. J. Hydraul. Res. 18 (3), 243–249. http://dx.doi.org/10.1080/00221688009499550.

Reid, I., Laronne, J.B., Powell, D.M., 1995. The Nahal Yatir bedload database: sediment dynamics in a gravel-bed ephemeral stream. Earth Surf. Proc. Land. 20, 845–857. http://dx.doi.org/10.1002/esp.3290200910.

Rickenmann, D., Turowski, J.M., Fritschi, B., Wyss, C., Laronne, J., Barzilai, R., Reid, I., Kreisler, A., Aigner, J., Seitz, H., Habersack, H., 2014. Bedload transport measurements with impact plate geophones: comparison of sensor calibration in different gravel-bed streams. Earth Surf. Proc. Land. 39 (7), 928–942. http://dx.doi.org/10.1002/esp.3499.

Schick, A.P., Lekach, J., 1993. An evaluation of two ten-year sediment budgets, Nahal Yael, Israel. Phys. Geogr. 14 (3), 225–238. http://dx.doi.org/10.1080/02723646.1993.10642477.

Sharma, K.D., 1996. Soil erosion and sediment yield in the Indian arid zone. In: Walling, D.E., Webb, B.W. (Eds.), Erosion and Sediment Yield: Global and Regional Perspectives, vol. 236. International Association of Hydrological Sciences Publication, Exeter, pp. 175–182.

Verstraeten, G., Bazzoffi, P., Lajczak, A., Radoane, M., Rey, F., Poesen, J., de Vente, J., 2006. Reservoir and pond sedimentation in Europe. In: Boardman, J., Poesen, J. (Eds.), Soil Erosion in Europe. John Wiley and Sons, Chichester, pp. 759–774.

Yamakoshi, T., Mathys, N., Klotz, S., 2009. Time-lapse video observation of erosion processes on the Black Marls badlands in the Southern Alps, France. Earth Surface Process. Land. 34 (2), 314–318. http://dx.doi.org/10.1002/esp.1701.